Biotechnology for Biofuels and Bioproducts

RESEARCH

Open Access

Kinetic modeling of multiple-strain artificial consortium to improve fengycin production of *Bacillus subtilis*

Shi-Long Jin[1,2†], Si-Yu Wei[1,3†], Geng-Rong Gao[1,3†], Lian-Bo Wei[1,2], Zhi-Xuan Li[1,2], Shao-Bo Zhang[1,2], Xin Liu[1,2], Xin-Hua Qi[1,3], Ming-Zhu Ding[1,3*], Jing-Sheng Cheng[1,3*] and Yong Zhang[1,2*]

Abstract

Background Artificial microbial consortium has been widely employed to improve the production of fengycin, a natural lipopeptide. Kinetic models are essential for understanding and predicting the dynamic behavior of metabolic systems, especially microbial consortia. Since the time evolution of metabolite concentrations and biomass is continuous and dynamic, systems of ordinary differential equations (ODEs) provide a natural and effective framework for capturing such interactions. In this work, a kinetic model based on ODEs was established to describe a multi-strain artificial consortium for fengycin synthesis, utilizing *Bacillus subtilis*, *Yarrowia lipolytica,* and *Corynebacterium glutamicum* as target strains.

Results The model captures microbial growth, intermediate metabolite formation, final product synthesis, and substrate consumption. It was successfully applied to analyze and interpret the cultivation data of target strains on various substrates. The model explicitly incorporates the accumulation of amino acids synthesized by *C. glutamicum*, the accumulation of fatty acids synthesized by *Y. lipolytica*, and the process in which *B. subtilis* utilized amino acids and fatty acids as partial precursors for fengycin production. The mathematical model ended up as a nonlinear ordinary differential system, which was solved with an adaptive step-size Runge–Kutta method, coupled with a genetic algorithm to roughly estimate the optimal model parameters associated with cellular growth, substrate consumption, and product level in fermentation broths.

Conclusions The numerical results of the kinetic model agreed well with experimental data, and all seven sets of experimental conditions were fitted with overall relative errors ranging from 7.4 to 15.1%. This kinetic modeling provided a meaningful tool for the rational design and construction of further artificial consortia.

Keywords Artificial consortium, Fengycin, Nonlinear ordinary differential equations, Optimization algorithm

†Shi-Long Jin, Si-Yu Wei and Geng-Rong Gao contributed equally to this work.

*Correspondence:
Ming-Zhu Ding
mzding@tju.edu.cn
Jing-Sheng Cheng
jscheng@tju.edu.cn
Yong Zhang
Zhang_Yong@tju.edu.cn
Full list of author information is available at the end of the article

Graphical Abstract

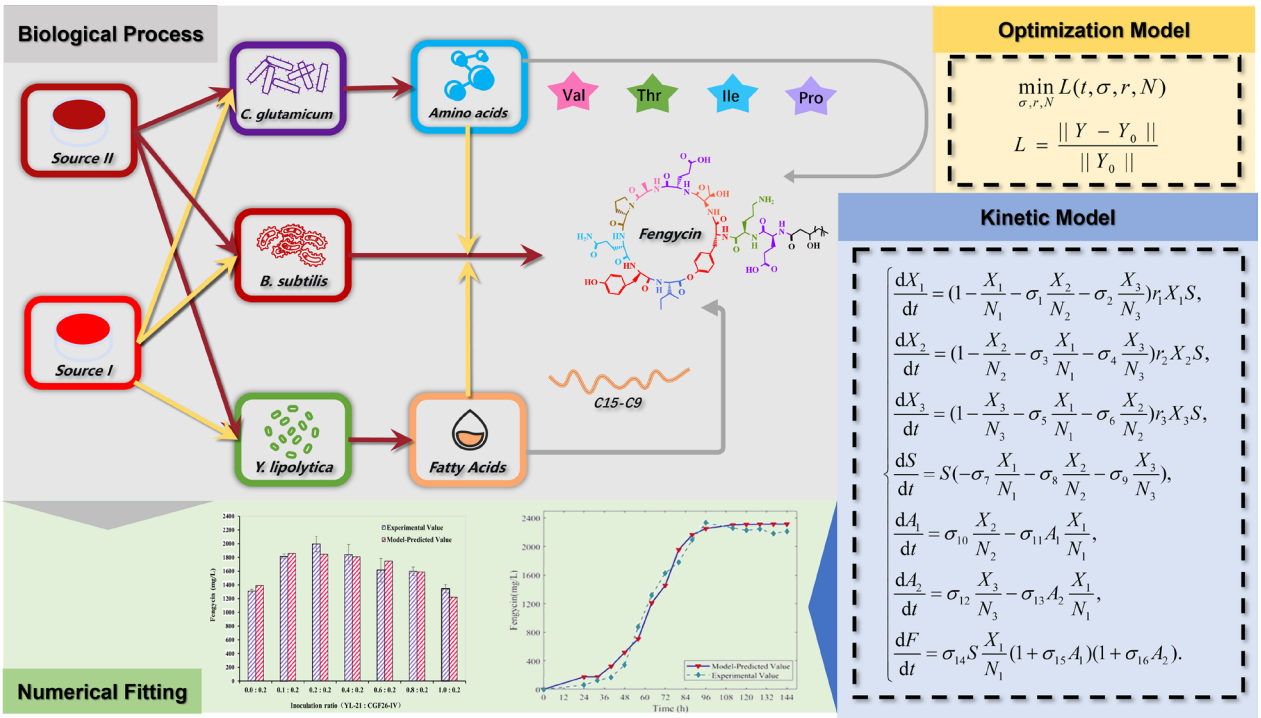

Background

Fengycin, a natural lipopeptide, is an important natural product with a wide range of biological activities and potential applications [1]. It is produced by *Bacillus* species and has been demonstrated to have various beneficial effects in agriculture, pharmaceuticals, and environmental applications [2–5]. As a biopesticide, fengycin inhibits the growth of plant pathogens, providing protection for crops against diseases. Additionally, fengycin exhibits pharmacological activities such as antibacterial, anticancer, and antioxidant properties, showcasing its broad potential in the field of biomedicine. Therefore, it is of great significance to promote the synthesis and production of fengycin.

Currently, the efforts to improve fengycin production primarily focus on fermentation optimization, where factors such as strain specificity, culture conditions, and extraction process substantially impact on titer and quality of fengycin [6–9]. To achieve an efficient production of fengycin, it is valuable to establish a kinetic model that comprehensively understands the synthesis mechanisms and key influencing factors of fengycin biosynthesis.

In recent years, the application of mathematical models and numerical algorithms in the field of biology has become increasingly widespread. Various types of mathematical models have been developed to describe different biological processes, including mechanistic modeling, stoichiometric modeling, and cybernetic modeling, among others [6, 7, 10–13]. For instance, Mandli [14] utilized a cybernetic modeling framework to investigate regulatory phenomena in microorganisms. Yasemi [15] studied a series of mathematical models concerning cell metabolism under steady-state conditions. Sidorenko [16] researched the dynamics of the recombinant *Saccharomyces cerevisiae* and the heterologous hantavirus protein. Wu [17] established a comprehensive mathematical model of quorum sensing (QS) regulation in co-culture and constructed an experimental combination of QS devices to evaluate the feasibility and optimality of its regulation of growth competition to achieve a high product titer in co-culture. However, research on the kinetic modeling of fengycin is relatively limited.

Therefore, we choose to investigate the fengycin production dynamics in artificial consortium via mathematical modeling, in the hope of finding better fermentation parameters to help optimize the fermentation process and improve fengycin production. We carry out a detailed analysis of the experimental process and finally develop a kinetic model to illustrate intricate interactions

between microorganisms and their metabolic activities. This model considers the growth kinetics of strains, the substrate consumption, the formation of intermediate metabolites, and the synthesis of fengycin.

By incorporating known biochemical reactions, the kinetic model was constructed for deducing the fengycin production in the artificial consortia of *C. glutamicum*, *Y. lipolytica*, and *B. subtilis*, and employed numerical methods and optimization algorithms to solve the kinetic model and estimate its unknown parameters.

Methods

Experimental design and method

This section mainly describes the principles and following constructs the kinetic model of fengycin production and corresponding wet experimental data collection methods.

Fengycin synthesis analysis

Fengycin was synthesized by *B. subtilis* via non-ribosomal polypeptide synthetase (NRPS) [6]. Amino acids and fatty acids, the structural precursors of fengycin, can promote the synthesis of fengycin by NRPS. Therefore, the amino acids produced by *C. glutamicum* and the fatty acids produced by *Y. lipolytica* were used to supply *B. subtilis* to produce fengycin, and a multiple-strain artificial consortium model was constructed.

The strains used in the experiments are as follows (Table 1):

- Fengycin producers: strains CGF-PG, CGF26-IV, and ΔrapJE (derivatives of *B. subtilis* CGF-P-02; strains engineered for fengycin biosynthesis) [19, 25–27].
- Amino acid producers: strains *C. glutamicum–PR* and cgb-11 (derivatives of *C. glutamicum*; strains designed for the production of fengycin structure-dependent precursor amino acids) [19, 25–28].
- Fatty acid producer: strain YL-21: (derivative of *Y. lipolytica* strain, engineered for the production of fengycin structure-dependent precursor fatty acids) [29].

In the artificial consortium, strains *C. glutamicum–PR* and cgb-11 can produce four different precursor amino acids. Strains CGF-PG, CGF26-IV, and ΔrapJE are all derivatives of *B. subtilis* CGF-P-02. Under the experimental conditions, the genetic modifications introduced in these strains showed negligible impact on their growth characteristics or fengycin production performance. Therefore, the mathematical model established by this study theoretically has extremely important guiding significance for mixed-strain systems involving derivatives of the *B. subtilis* CGF26 series.

Preparation of microbial culture medium

The composition of the fermentation medium was a key factor in microbial fermentation culture, especially the selection of carbon source and nitrogen source and their composition ratio [18]. Medium Cal18-7, the optimum medium for producing fengycin in an artificial consortium [19], contains 40.0 $g{\cdot}L^{-1}$ maltodextrin, 10.0 $g{\cdot}L^{-1}$ sucrose, 30.0 $g{\cdot}L^{-1}$ yeast extract, 1.3 $g{\cdot}L^{-1}$ $MgSO_4{\cdot}7H_2O$, 20.0 $g{\cdot}L^{-1}$ $Na_2HPO_4{\cdot}12H_2O$, 6.7 $g{\cdot}L^{-1}$ $Na_2MoO_4{\cdot}2H_2O$, 3.0 $g{\cdot}L^{-1}$ KH_2PO_4, 5.0 $g{\cdot}L^{-1}$ $(NH_4)_2SO_4$, 0.02 $g{\cdot}L^{-1}$ $FeSO_4{\cdot}7H_2O$, 0.02 $g{\cdot}L^{-1}$ $MnSO_4{\cdot}H_2O$, 0.45 $mg{\cdot}L^{-1}$ vitamin B1, and 0.05 $mg{\cdot}L^{-1}$ vitamin B7. The kinetic model employed in this study was also established based on the medium. Subsequent microbial consortium media were all formulated based on this basal medium with appropriate modifications.

Measurement of biomass

The microbial biomass at different times of the fermentation solution was detected by ultraviolet spectrophotometer at 600 nm, and the microbial growth curve was drawn.

Table 1 Strains used in this study

Strains	Characteristics	Refs.
CGF-PG	*B. subtilis* 168 derivate, P43-*sfp-degQ*, Δ*srfAB-AC*, Δ*pksBCDE*, P_{veg}-*fenC*, P43-*accBC*, P43-*fabHB*, Δ*tapA-sipW-tasA*, Δ*epsAB*, Δ*spoIIIE*, PfbaA-*opuE*, C2up-*egfp*	[19]
CGF26-IV	*B. subtilis* 168 derivate, P43-sfp-degQ, Δ*srfAB-AC*, Δ*pksBCDE*, P_{veg}-*fenC*, P43-*accBC*, P43-*fabHB*, Δ*tapA-sipW-tasA*, Δ*epsAB*, Δ*spoIIIE*, *PfbaA-livH*	[19]
C. glu-PR	*C. glutamicum* ATCC 13032 derivate, Δ*putA*, a mutation in the *proB*, P_{tuf}- *mcherry*	[19]
ΔrapJE	*B. subtilis* 168 derivate, Δ*pksBCDE*, P_{veg}-*fenC*, P43-*accBC*, P43-*fabHB*, Δ*tapA-sipW-tasA*, Δ*epsAB*, Δ*spoIIIE*, PfbaA-*opuE*, PsrfA-*ppsA*, PsrfA-*RE3-ppsA*, Δ*rapJ*, Δ*rapE*	[27]
Cgb-11	*C. glutamicum ATCC 13032 derivate*, Δ*pck*, Δ*ddh*, Δ*lysE*, Δ*ilvA*, Δ*metX*, Δ*putA*, *proB mutation*, *Ptrc-ilvBN*	[28]
YL-21	ATCC 201249 derivate, Δ*Ku70::PTEFin-VHb*, Δ*PHD1*, Δ*PAH1*, Δ*LRO1*, Δ*FAA1*	[29]

Measurement of fengycin concentration

The fengycin was quantitatively determined by high-performance liquid chromatography (HPLC). The sample size was 10.0 L. The chromatography was performed on a C18 reverse-phase column (4.6 mm × 150 mm, 5 μm) with 50.0% acetonitrile and 50.0% pure water (containing 1.0% trifluoroacetic acid) as mobile phases [18].

Fermentation in Erlenmeyer flasks

The activated microbial seeds were inoculated into a 500-mL Erlenmeyer flask containing 80 mL of the Cal18-7 medium and cultured at 30 °C and 180 rpm for 72 h. The fengycin was extracted from the supernatant of the fermentation broth after 72 h for quantitative measurement.

Fermentation in bioreactors

For scale up, the activated microbial seeds were inoculated into a 5.0-L bioreactor containing 3.5 L of the Cal18-7 medium and cultured at 30 °C and 300 rpm. The airflow rate was maintained at 2.0 $L \cdot min^{-1}$. Carbon and nitrogen sources were added during the fermentation process at 32, 56, and 72 h when the pH increased.

Construction of the kinetic model

In this section, a mathematical model will be established to describe the biological process. The concentration of fengycin will serve as the primary research target, and a comprehensive kinetic model will be formulated to capture the kinetics of microbial growth, substrate consumption, and product formation throughout the fermentation process. In the following, we take the mixed-culture experiment of *B. subtilis*, *C. glutamicum*, and *Y. lipolytica* as an example to illustrate the process of constructing the kinetic model.

Basic principles and assumptions

In the experimental process, our focus will be on extracting the key biological reactions while considering the remaining biological reactions as relatively weak or negligible in terms of their impact on the specific objectives of our study.

By simplifying the model and focusing on the critical factors that influence the system's kinetics, we streamlined our analysis and concentrated our efforts on the most significant aspects. It is crucial to note that this simplification is well justified, as it allows us to capture the essential kinetics while minimizing the inclusion of negligible or irrelevant processes.

The complete biological process intended to simulate is as follows. In the fermentation medium, maltodextrin (MD) and sucrose were utilized as the primary carbon sources. Initially, *C. glutamicum* was inoculated in advance to facilitate amino acids' accumulation. Subsequently, *B. subtilis* was inoculated for fengycin production. Similarly, pre-inoculation with *Y. lipolytica* could promote the accumulation of fatty acids. We established a similar dynamic model for *Y. lipolytica* and *C. glutamicum*, and in the two-strain artificial consortium, we used *C. glutamicum* as a representative for illustration. In the three-strain artificial consortium, *C. glutamicum* and *Y. lipolytica* were pre-inoculated at intervals to ensure the accumulation of amino acids and fatty acids, as shown in Fig. 1.

Construction of the kinetic model for the two-strain artificial consortium

In the course of the two-strain artificial consortium, the following variables were extracted and utilized to establish a mathematical model:

- $X_1(t)$: The amount of strain *B. subtilis* at time t (OD_{600}).
- $X_2(t)$: The amount of strain *C. glutamicum*/*Y. lipolytica* at time t (OD_{600}).
- $S_1(t)$: The amount of sucrose at time t (g/L).
- $S_2(t)$: The amount of MD (maltodextrin) at time t (g/L).
- $A(t)$: The amount of amino acids/(fatty acids)) at time t (g/L).
- $F(t)$: The amount of fengycin at time t (mg/L).

These variables capture the essential parameters and components involved in the two-strain artificial consortium and were used to establish a comprehensive mathematical model that describes the kinetics and interactions between them.

Microbial growth model

Based on the growth characteristics of bacteria in the artificial consortium, the Monod equation [20] and the Logistic equation [21] are commonly used to describe the basic bacterial growth kinetics. The Monod equation describes the relationship between the specific growth rate of the bacterial population and the substrate concentration. However, this equation is more suitable for single-species systems where other limiting factors are not present. Based on the feedback from numerical simulations and considering that the focus of this study is a mixed bacteria system, we will start with the Logistic equation and incorporate modifications to account for interspecies interaction. This approach allows us to construct a growth kinetics model for a mixed microbial

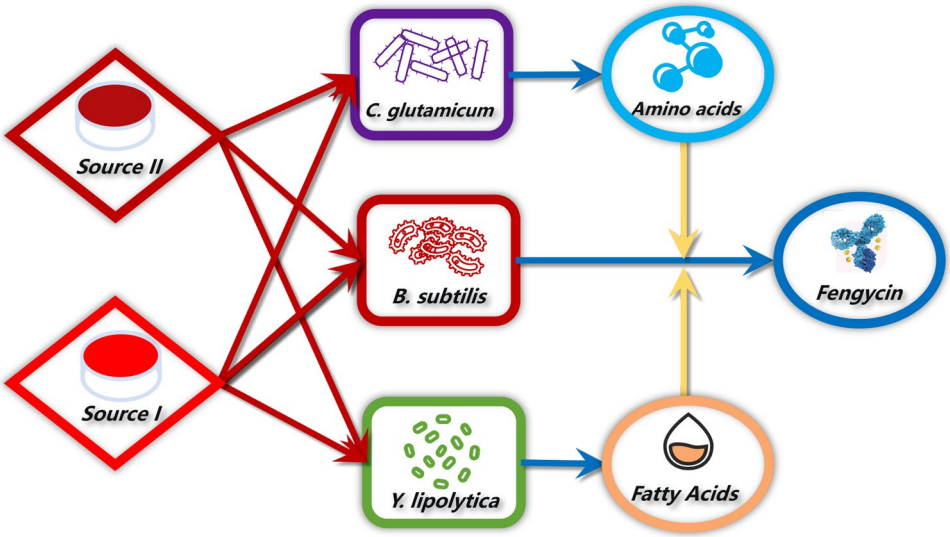

Fig. 1 Schematic diagram: synthesis route of fengycin. Two carbon sources (e.g., sucrose and maltodextrin) are utilized by microbial consortia to generate intermediate metabolites, which subsequently participate in fengycin biosynthesis. Red arrows indicate substrate consumption, blue arrows denote metabolite production, and yellow arrows represent pathways that promote the synthesis of fengycin

system under limiting substrate conditions. The classical form of the logistic model is as follows:

$$\frac{1}{X}\frac{\mathrm{d}X}{\mathrm{d}t} = r\left(1 - \frac{X}{N}\right), \tag{1}$$

where X denotes the bacteria population size, r represents the population growth rate, and N is the carrying capacity of the environment.

Considering that substrates in the bacterial fermentation process are limited and continuously consumed, logistic model (1) should be modified as shown in logistic model (2), with S_i denoting the substrates and r_i indicating the respective bacterial growth coefficients for each substrate. This modified equation incorporates the limitation of substrate availability in the bacterial fermentation process and considers the influence of different substrates on the growth rates of bacteria. It is worth mentioning that this equation can be readily extended to multi-strain consortiums; however, one should be aware of the challenges in parameter optimization arising from the high dimensionality:

$$\frac{1}{X}\frac{\mathrm{d}X}{\mathrm{d}t} = \left(1 - \frac{X}{N}\right)\sum_i r_i S_i. \tag{2}$$

During the experimental process, bacterial growth can be divided into two stages. The first stage involves the inoculation of *C. glutamicum* or *Y. lipolytica* in advance, representing a single-species system. In this stage, we can start with the logistic model (2). Similarly, after the inoculation of *B. subtilis* to establish a mixed bacteria system, we can start from the interspecies interaction model (3). In this model, considering the limited substrates in the medium, a similar modification is applied to the model, resulting in the following form:

$$\begin{cases} \frac{\mathrm{d}X_1}{\mathrm{d}t} = \left(1 - \frac{X_1}{N_1} - \sigma_1\frac{X_2}{N_2}\right)X_1(r_1S_1 + r_2S_2), \\ \frac{\mathrm{d}X_2}{\mathrm{d}t} = \left(1 - \frac{X_2}{N_2} - \sigma_2\frac{X_1}{N_1}\right)X_2(r_3S_1 + r_4S_2), \end{cases} \tag{3}$$

where N_1 and N_2 represent the environmental carrying capacities, while σ_1 and σ_2 represent the competition coefficients. The coefficients r_1, r_2, r_3, and r_4 represent the growth coefficients of *C. glutamicum* or *Y. lipolytica* and *B. subtilis* with respect to two different substrates. This modified model takes into account the limitation of substrate availability in the medium and the growth coefficients of *C. glutamicum* and *B. subtilis* with respect to different substrates.

The proposed model effectively captures the rapid growth in the early and middle stages of the fermentation process, as well as the growth inhibition caused by various inhibitory conditions in the later stages.

Substrate consumption model

Within the entire medium, the carbon sources are primarily sucrose and maltodextrin, serving three main purposes: (1) sustaining the normal metabolic activities of bacteria; (2) fueling the growth and reproduction of bacteria; and (3) supporting the production of desired products. In accordance with the notation used previously, the consumption of these two carbon sources can be modeled as model (4) using the following equations:

$$\begin{cases} \frac{dS_1}{dt} = S_1\left(-\sigma_3\frac{X_1}{N_1} - \sigma_4\frac{X_2}{N_2}\right), \\ \frac{dS_2}{dt} = S_2\left(-\sigma_5\frac{X_1}{N_1} - \sigma_6\frac{X_2}{N_2}\right), \end{cases} \tag{4}$$

where S_1 and S_2 denote the concentrations of sucrose and maltodextrin, respectively, and X_1 and X_2 denote the population sizes of two strains. The coefficients σ_3, σ_4, σ_5, and σ_6 correspond to the consumption rates of the two carbon sources by these two strains.

Kinetic modeling of intermediate and final products

As shown in Fig. 1, during the growth of *C. glutamicum* or *Y. lipolytica*, amino acids or fatty acids are metabolically produced and subsequently consumed by *B. subtilis*, thereby accelerating the synthesis of fengycin. To describe the relationship between the amino acids (or fatty acids) production rate and the growth of *C. glutamicum* (or *Y. lipolytica*), we employ the widely used Leudeking–Piret equation as a generic model. Considering the unknown coupling relationship between *C. glutamicum* growth and amino acids production, we adopt model (5) with the best numerical results for modeling purposes. In a similar manner, the same modeling framework is employed to characterize the consumption of amino acids by *B. subtilis*. In the model, σ_7 denotes the amino acids production coefficient of *C. glutamicum*, while σ_8 represents its amino acids consumption coefficient:

$$\frac{dA}{dt} = \sigma_7\frac{X_2}{N_2} - \sigma_8 A\frac{X_1}{N_1}. \tag{5}$$

Regarding fengycin, it is synthesized by *B. subtilis* utilizing the substrates present in the medium, facilitated by the effect of amino acids and fatty acids. In this context, we adopt a modeling strategy analogous to that used for amino acid synthesis, accounting for both substrate limitation and the enhancement effect exerted by amino acids. Consequently, model (6) is derived to describe the kinetics of fengycin production, where σ_9 denotes the synthesis coefficient of *B. subtilis* for fengycin production, and σ_{10} quantifies the enhancement effect of amino acids or fatty acids on fengycin biosynthesis:

$$\frac{dF}{dt} = \sigma_9\frac{X_1}{N_1}(1 + \sigma_{10}A)(S_1 + S_2). \tag{6}$$

Based on the three components described above, we have constructed a comprehensive kinetic model for fengycin biosynthesis. Specifically, the model comprises two sets of ODEs: the first set model (7) describes the monoculture system in which *C. glutamicum* is pre-inoculated alone, and the second set model (8) represents the co-culture system after the inoculation of *B. subtilis* for fengycin synthesis. The model encompasses a total of 16 parameters, denoted as r_i, N_j, σ_k, which capture the functional relationships pertaining to bacterial growth, substrate consumption, and synthesis of the product, among other aspects.

Step I: The monoculture system of *C. glutamicum*

$$\begin{cases} \frac{dX_2}{dt} = \left(1 - \frac{X_2}{N_2}\right)X_2(r_3S_1 + r_4S_2) \\ \frac{dS_1}{dt} = S_1\left(-\sigma_4\frac{X_2}{N_2}\right), \\ \frac{dS_2}{dt} = S_2\left(-\sigma_6\frac{X_2}{N_2}\right), \\ \frac{dA}{dt} = \sigma_7\frac{X_2}{N_2}, \end{cases} \tag{7}$$

Step II: The co-culture system with *B. subtilis* and *C. glutamicum*

$$\begin{cases} \frac{dX_1}{dt} = \left(1 - \frac{X_1}{N_1} - \sigma_1\frac{X_2}{N_2}\right)X_1(r_1S_1 + r_2S_2), \\ \frac{dX_2}{dt} = \left(1 - \frac{X_2}{N_2} - \sigma_2\frac{X_1}{N_1}\right)X_2(r_3S_1 + r_4S_2), \\ \frac{dS_1}{dt} = S_1\left(-\sigma_3\frac{X_1}{N_1} - \sigma_4\frac{X_2}{N_2}\right), \\ \frac{dS_2}{dt} = S_2\left(-\sigma_5\frac{X_1}{N_1} - \sigma_6\frac{X_2}{N_2}\right), \\ \frac{dA}{dt} = \sigma_7\frac{X_2}{N_2} - \sigma_8 A\frac{X_1}{N_1}, \\ \frac{dF}{dt} = \sigma_9\frac{X_1}{N_1}(1 + \sigma_{10}A)(S_1 + S_2). \end{cases} \tag{8}$$

Remark: A similar variant of Eq. (7) can also be formulated to describe the scenario where *B. subtilis* is pre-inoculated alone.

Construction of the kinetic model for the three-strain artificial consortium

In the course of the three-strain artificial consortium, the following variables are extracted and utilized to establish a mathematical model:

- $X_1(t)$: The amount of strain *B. subtilis* at time t (OD_{600})
- $X_2(t)$: The amount of strain *C. glutamicum* at time t (OD_{600})
- $X_3(t)$: The amount of strain *Y. lipolytica* at time t (OD_{600})
- $S(t)$: The amount of carbon source which is the sum of sucrose and MD at time t (g/L)
- $A_1(t)$: The amount of amino acids at time t (g/L)
- $A_2(t)$: The amount of fatty acid at time t (g/L)
- $F(t)$: The amount of fengycin at time t (mg/L)

To reduce the parameter number and to simplify the numerical optimization process, the difference between the two carbon sources is ignored and considered as a whole. The overall approach is consistent with the two-strain artificial consortium.

By employing a similar framework encompassing bacterial growth, substrate consumption, and the production and utilization of intermediate and final metabolites, and under the assumption that *Y. lipolytica* and *C. glutamicum* exert no direct influence on the dynamics of fatty acids, we constructed the following ordinary differential equations (ODEs):

$$\begin{cases} \frac{dX_1}{dt} = \left(1 - \frac{X_1}{N_1} - \sigma_1\frac{X_2}{N_2} - \sigma_2\frac{X_3}{N_3}\right) r_1 X_1 S, \\ \frac{dX_2}{dt} = \left(1 - \frac{X_2}{N_2} - \sigma_3\frac{X_1}{N_1} - \sigma_4\frac{X_3}{N_3}\right) r_2 X_2 S, \\ \frac{dX_3}{dt} = \left(1 - \frac{X_3}{N_3} - \sigma_5\frac{X_1}{N_1} - \sigma_6\frac{X_2}{N_2}\right) r_3 X_3 S, \\ \frac{dS}{dt} = S\left(-\sigma_7\frac{X_1}{N_1} - \sigma_8\frac{X_2}{N_2} - \sigma_9\frac{X_3}{N_3}\right), \\ \frac{dA_1}{dt} = \sigma_{10}\frac{X_2}{N_2} - \sigma_{11}A_1\frac{X_1}{N_1}, \\ \frac{dA_2}{dt} = \sigma_{12}\frac{X_3}{N_3} - \sigma_{13}A_2\frac{X_1}{N_1}, \\ \frac{dF}{dt} = \sigma_{14}S\frac{X_1}{N_1}(1 + \sigma_{15}A_1)(1 + \sigma_{16}A_2). \end{cases} \tag{9}$$

The model (9) comprises 22 parameters, which describe a mixed system containing *Y. lipolytica*, *C. glutamicum*, and *B. subtilis*.

Numerical solution and parameter optimization

In this section, we employed a genetic algorithm [22, 23] combined with the adaptive-step Runge–Kutta method [24] to optimize the parameters so as to minimize the simulation error.

Numerical solution

We employ an adaptive Runge–Kutta method to numerically solve the ODEs. The variable-step Runge–Kutta method adjusts the step size dynamically for better efficiency and produces a reliable solution by controlling numerical tolerance parameters.

System (model 7) is first solved numerically till the inoculation time, then the solution is used as the initial value for the subsequent (model 8) system. Following the same way, we obtain numerical solutions at the given experimental time. The three-strain artificial consortium is solved similarly.

Parameter optimization

Denote the experimental data by Y_0, which corresponds to representing measured concentrations of fengycin at different times or initial values. Denote the numerical solution as Y. It is important to note that Y is related to all the unknown parameters σ, r, k in the model, that is, $Y = Y(\sigma, r, k)$.

To better capture the biological processes in the medium, we aim to find a set of unknown parameters that yield numerical results $Y(\sigma, r, k)$ that closely match the experimental results Y_0. This will facilitate a better understanding of the entire biological process and provide guidance for future experiments:

$$\min_{\sigma,r,N} L(t, \sigma, r, N). \tag{10}$$

Therefore, we establish an optimization model with (model 10) as the objective function. In this case, we choose the relative error in the norm as the measure of closeness between $Y(\sigma, r, k)$ and Y_0 as:

$$L = ||Y - Y_0||/||Y_0||. \tag{11}$$

In the numerical experiments, we used two commonly adopted error measures: the ∞-norm and the L_2-norm. For a vector $Y = (y_1, y_2, y_3, \ldots y_N)$, its ∞-norm and the L_2-norm can be defined as follows:

$$||Y||_\infty = \max_i |Y_i|, \; ||Y||_2 = \left(\sum_{i=1}^{N} y_i^2\right)^{1/2}. \tag{12}$$

In the numerical analysis, the L2-norm reflects the fitting performance using the average squared deviation between the model predictions and the experimental data, while the ∞-norm is the maximum deviation. From this perspective, the two norms together provide a good evaluation of the point-wise and averaged accuracy of the fitting.

To optimize the parameters of the kinetic model and improve its accuracy in capturing the dynamics between limited substrates and bacterial populations, we employed a genetic algorithm (GA) as an efficient optimization technique. The GA is a heuristic search algorithm inspired by the process of natural selection and evolution. It has been widely used in various optimization problems, including parameter estimation in mathematical models.

It should be noted that the stability of the parameter estimates is theoretically supported by the well-posedness of the underlying ordinary differential equation theory, which ensures that small perturbations in parameters do not lead to unstable solutions.

During the optimization process, we employ the MATLAB's Optimization Toolbox, a specialized toolkit developed by MathWorks and widely used for implementing genetic algorithms in complex optimization tasks. The optimization settings are carefully tuned, including selection, crossover, mutation strategies, population control, and evolutionary mechanisms, to ensure stable convergence and effective exploration of the solution space. In the calculation of the objective function, we take the two-strain artificial consortium as an example to provide the calculation process of L as Algorithm 1. Through multiple rounds of optimization trials, the algorithm yields satisfactory results.

Algorithm 1 Objective Function Calculation L in two-strain artificial consortium

Input: Experimental data Y_0

Initial conditions **For** (model 7) $X_2\, S_1\, S_2\, A$

Initial conditions **For** (model 8) X_1

Parameters σ, r, k

Time $T_1\, T_2$

Output: Objective Function value L under Parameters σ, r, k.

Steps:

For the *i-th* **experimental group** (X_1, X_2, T_1, T_2)

  Set initial values (X_2, S_1, S_2, A)

  Solve (model 7) **from** t=0 **to** t= T_1

  →Obtain **values** (X_2, S_1, S_2, A) at t= T_1

  Use (X_1, X_2, S_1, S_2, A, F_2) as new **initial values**

  Solve (model 8) **from** t=0 **to** t= T_2

  Extract **final product value** F_i **as** Y_i

End For

Compute objective function L

$$L = \| Y - Y_0 \| / \| Y_0 \|$$

Return L

Remark: In fact, we may also consider parameter optimization methods based on optimal control theory (OCT). The parameters can be treated as control variables, with the objective of minimizing the error between the numerical solutions and the experimental data as (10). However, this problem is essentially nonlinear, and its smoothness and convexity cannot be guaranteed, so we employed GA for the solution. In the future, gradient-based optimization methods may be considered to improve efficiency.

Results

Two-strain artificial consortium of strains CGF-PG and C. glu-PR

Numerical simulation in Erlenmeyer flasks

The inoculation time and initial ratio of artificially microbial consortia affect the growth rate of each strain and the interactions among microbial populations as well as their metabolic capacity. In our previous study, an artificial consortium of strains *C. glu*-PR and CGF-PG was constructed to investigate the effects of different inoculation ratios and fermentation times on the fengycin production [19, 25].

We used our previous experimental results of Gao et al. [19, 25] as a data source. In the numerical simulation aspect, we represented different co-culture ratios by changing the initial values of the ODEs. By solving the corresponding ODEs separately at different time intervals, the delayed inoculation of the two strains was captured. For the data in the objective function for model optimization, we mainly focused on fitting the data of fengycin production at inoculation time and initial ratio of microbial co-cultures.

In our numerical simulations, the model achieved a fitting accuracy of 9.0% in ∞-norm sense when compared with experimental data on inoculation time and initial ratio. The simulation results are as shown in Fig. 2. In this numerical experiment, the overall fitting error of our model remains relatively low, demonstrating good agreement with both types of experimental data.

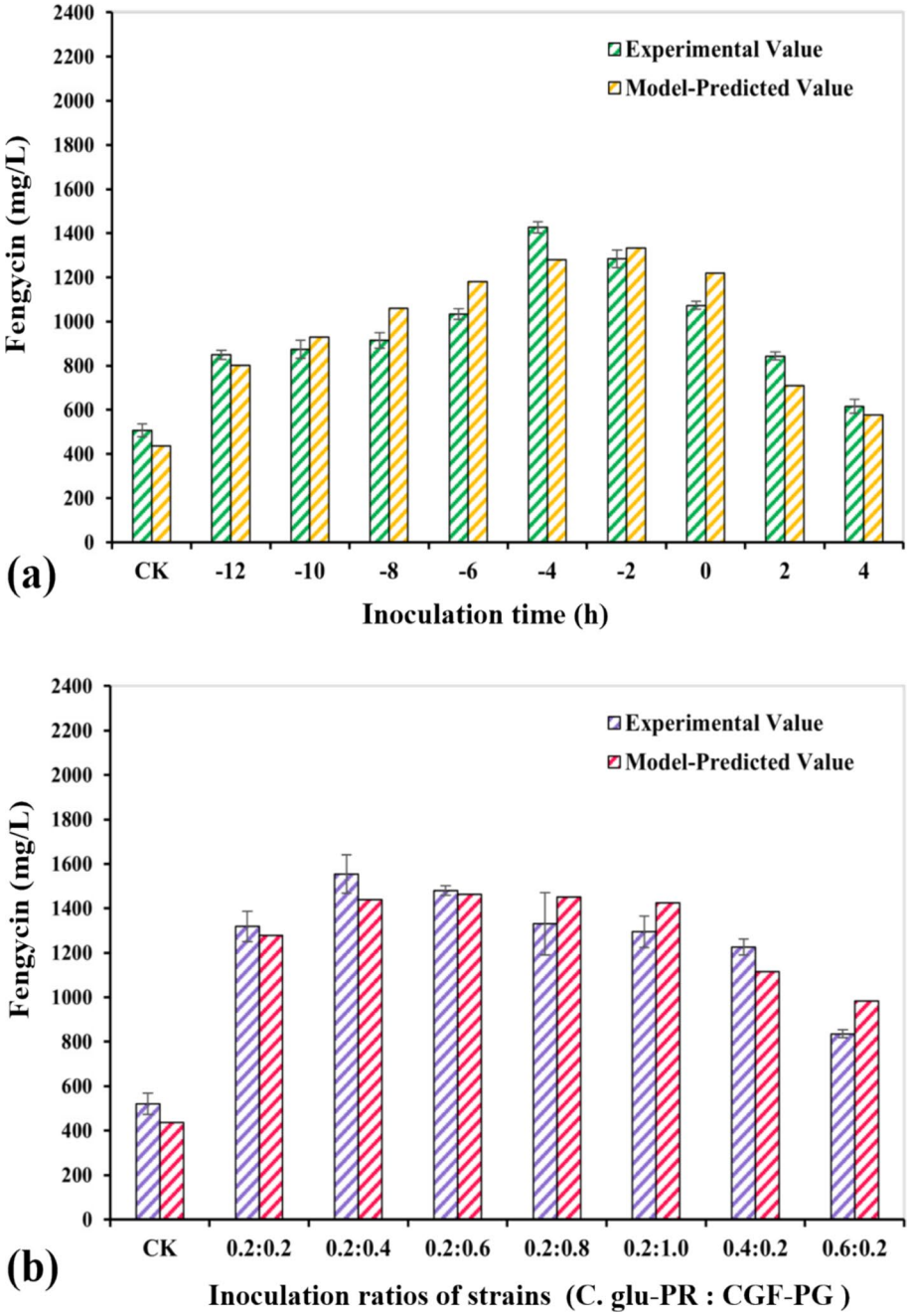

Fig. 2 Simulation results of fengycin production in Erlenmeyer flask under the co-culture of strains C. glu-PR and CGF-PG. **a** Effects of inoculation times, **b** effects of inoculation ratios. Data are presented as mean ± SD from three biologically independent samples

Under the optimal culture conditions, the fitting error achieved 15% in L_2-norm sense for the kinetic experimental data. These results correspond to the optimal set of kinetic parameters identified by the mathematical model. Upon closer analysis, the model exhibited better performance in simulating the trend of mid-to-late stages and the final production, as shown in Fig. 3. Considering the fermentation kinetics, if we focus solely on the logarithmic growth phase, decay phase, and steady-state phase, while disregarding the slow growth during the lag phase, and only fit the fengycin dynamics data after 48 h and the final product data for different co-culture ratios, the relative error was reduced to around 12.0%.

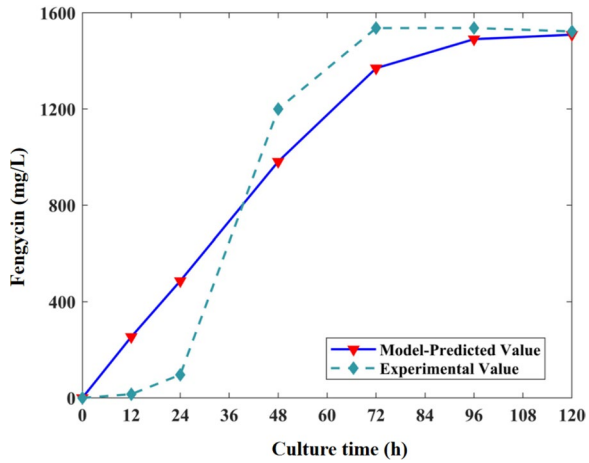

Fig. 3 Simulation results of fengycin production kinetics in Erlenmeyer flask under the co-culture of strains CGF-PG and C. glu-PR

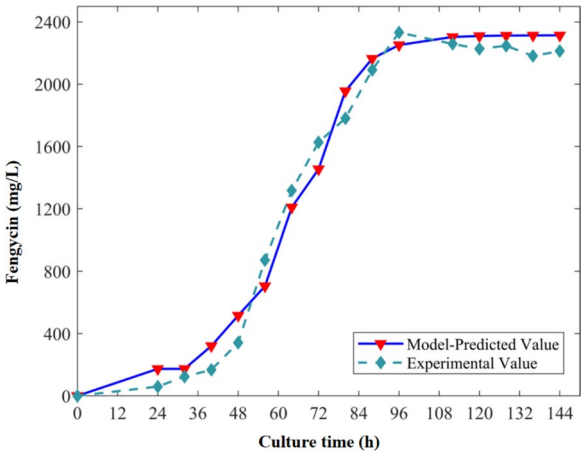

Fig. 4 Fengycin production kinetics simulation in the bioreactor cultivation of strains CGF-PG and C. glu-PR

For this experiment, the shake flask cultivation represents a relatively small-scale setup, which is more susceptible to environmental fluctuations and sampling disturbances. As a result, the relative error tends to be higher compared to larger-scale or more controlled systems.

Numerical simulation in bioreactor

In the same way, we used the experimental results of Gao et al. [19, 25] in the bioreactor as the data source for the numerical simulations; the experimental setup in the bioreactor is similar to that in the Erlenmeyer flasks. However, there are three main differences. Firstly, the scale of the experiment is larger in the bioreactor, leading to a significant reduction in experimental errors caused by sampling. Secondly, only a single mixing ratio of 0.2:0.4 was tested in the bioreactor, and no other ratios were investigated. Additionally, considering substrate consumption, feeding of additional nutrients is performed at three time points: 32 h, 56 h, and 72 h, during the fermentation process in the bioreactor. The total volume of the feeds was 500 mL, containing 210.0 g/L maltodextrin, 70.0 g/L sucrose, 210.0 g/L yeast extract, and 17.5 g/L $(NH4)_2SO_4$. Each replenishment was 166.67 mL of the feeds.

The experimental data of Gao et al. [19, 25] display the production kinetics of fengycin. Based on these data, we numerically simulated the fengycin production kinetics in a bioreactor. During the numerical solution of the kinetic model, we incorporate segmented treatment of the mixed microbial ODEs (9) based on the previous handling approach. At each specific time point, the model (9) is segmented and treated separately. The concentrations of corresponding carbon sources are updated at each feeding time point, and these updated concentrations are used as new initial values for solving the equations within that segment.

This process continues for each segment until the complete solution of the entire kinetic model is obtained. And in the model fitting process, we focus on fitting the kinetic data of fengycin production in the mixed microbial system.

The overall model fitting of the data from the fermenter shows a relative error of approximately 7.5% in ∞-norm sense. Figure 4 demonstrates a close agreement between the simulated and actual curves, indicating a good fit of the model, and clearly shows a significant increase in the fengycin production at several time points of supplementary feeding, indicating a successful fit of the fengycin production dynamics.

Two-strain artificial consortium of strains ΔrapJE and Cgb-11

The recombinant *B. subtilis* strain ΔrapJE was derived from the parental strain CGF-P-02 through promoter replacement and gene knockout [26, 27]. In the co-culture system with strains ΔrapJE and Cgb-11, strain Cgb-11 could produce high amino acid levels (Thr, Pro, Val, and Ile) and provide the necessary precursor for fengycin synthesis. This study focuses on the effects of inoculation time and initial ratio of strains ΔrapJE and Cgb-11 on fengycin production.

In the inoculation time experiment, strain ΔrapJE was added to the medium at 0 h, while strain Cgb-11 was inoculated at various time points: −4 h (4 h in advance), −2 h, 0 h, +2 h, and +4 h relative to strain

ΔrapJE inoculation. In the inoculation ratio experiment, strains C. glu and ΔrapJE were inoculated into the medium at OD_{600} values of 0.8:0.2, 0.6:0.2, 0.4:0.2, 0.2:0.2, 0.2:0.4, 0.2:0.4, 0.2:0.6, and 0.2:0.8 at the corresponding inoculation time.

The model fitting for this experimental dataset yielded an overall error of approximately 13.7% in ∞-norm sense (Fig. 5), indicating a satisfactory agreement between simulation and experimental results. In addition, the relative errors of the control check groups from both datasets demonstrate that the model captures this system reasonably well and meets the expected level of accuracy.

Three-strain artificial consortium of strains Cgb-11, YL-21, and CGF26-IV

The impacts of inoculation ratios and time on fengycin production among strains Cgb-11, YL-21, and CGF26-IV was explored in our previous study [25, 28], and we used the experimental results as a data source here. The experimental design comprises two sets of two-strain artificial consortia: one involving strains Cgb-11 and

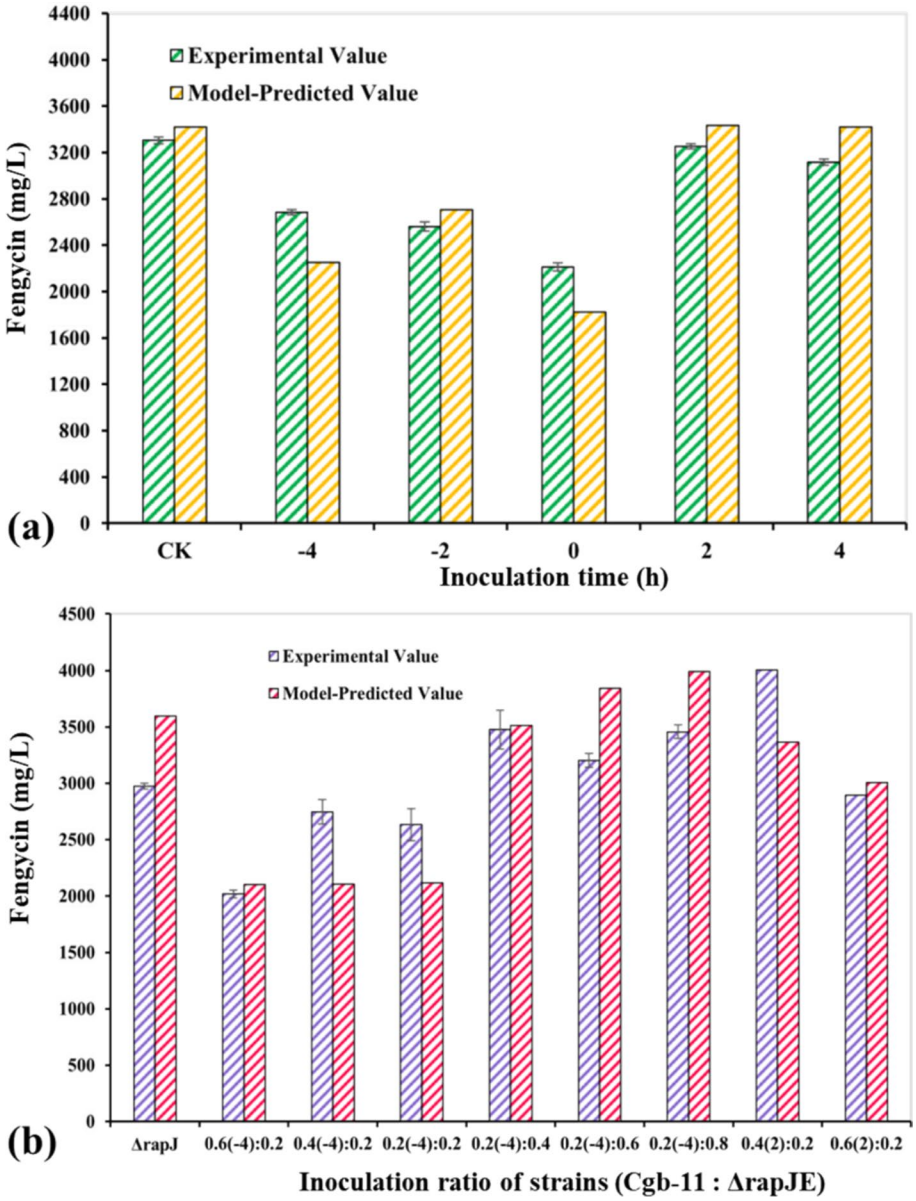

Fig. 5 Simulation results of fengycin production under the co-culture of strains Cgb-11 and ΔrapJE. a Effects of inoculation times, **b** effects of inoculation ratios. Data are presented as mean ± SD from three biologically independent samples

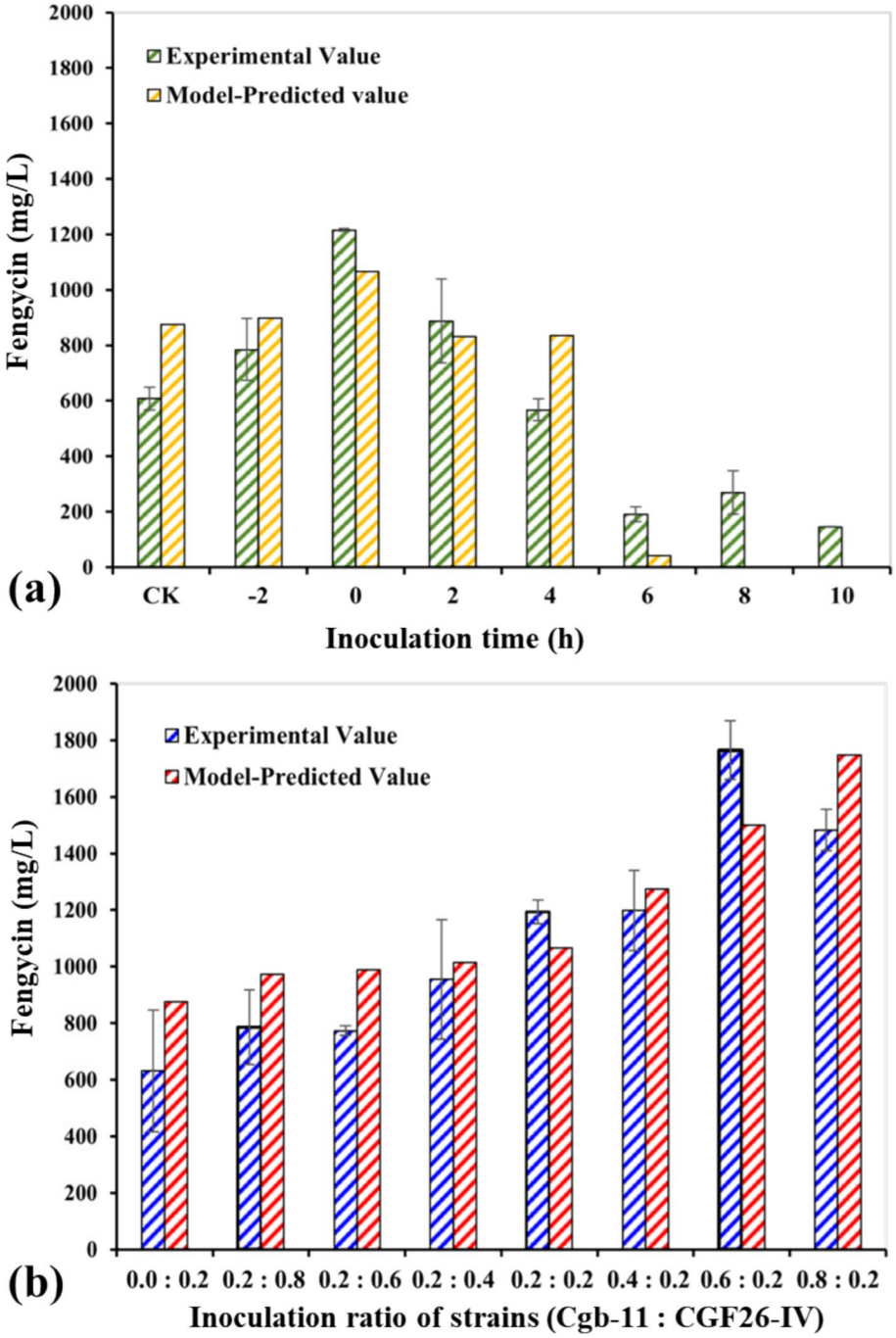

Fig. 6 Simulation results of fengycin production under the co-culture of strains Cgb-11 and CGF26-IV. **a** Effects of inoculation times, **b** effects of inoculation ratios. Data are presented as mean ± SD from three biologically independent samples

CGF26-IV, and the other involving strains YL-21 and CGF26-IV. In addition, a three-strain artificial consortium composed of strains Cgb-11, YL-21, and CGF26-IV was also constructed and investigated.

Two sets of two-strain artificial consortium

In this set of experiments, two sets of two-strain artificial consortium experiments were conducted initially. These experiments involved the artificial consortium system of strains CGF26-IV with Cgb-11 and YL-21, respectively, to investigate the optimal inoculation time and ratio. It

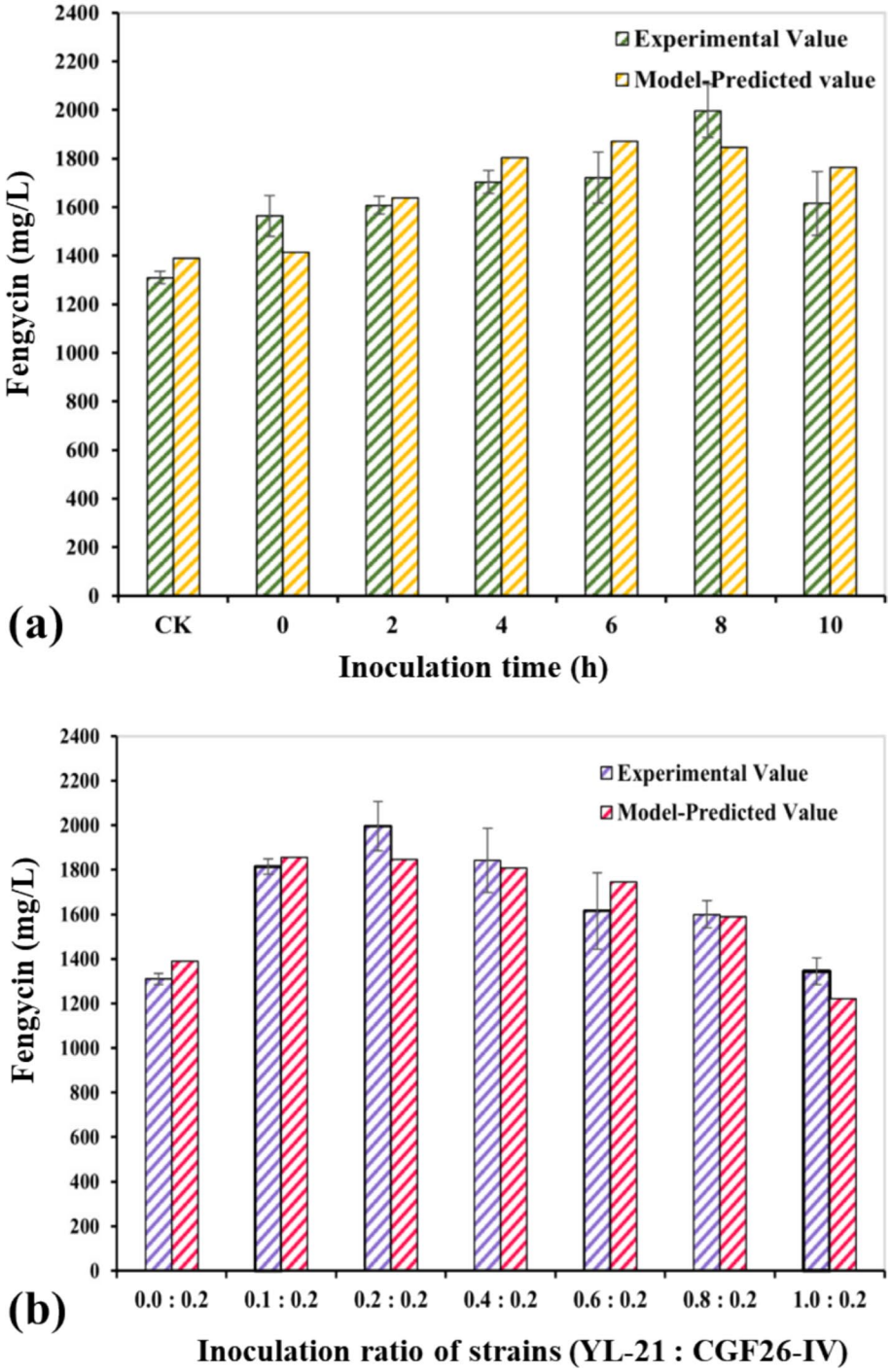

Fig. 7 Simulation results of fengycin production under the co-culture of strains YL-21 and CGF26-IV. Data are presented as mean ± SD from three biologically independent samples. **a** Effects of inoculation times, **b** effects of inoculation ratios

is noteworthy that, to maintain consistency with the subsequent three-strain artificial consortium, the two-strain artificial consortium system used here undergoes certain modifications based on models (8) and (9). Similarly, both carbon sources are treated as a whole in this case.

The fitting performance of the Cgb-11 and CGF26-IV two-strain artificial consortium model reached a relative error of 15.1% in ∞-norm sense, and the YL-21 and CGF26-IV two-strain artificial consortium model

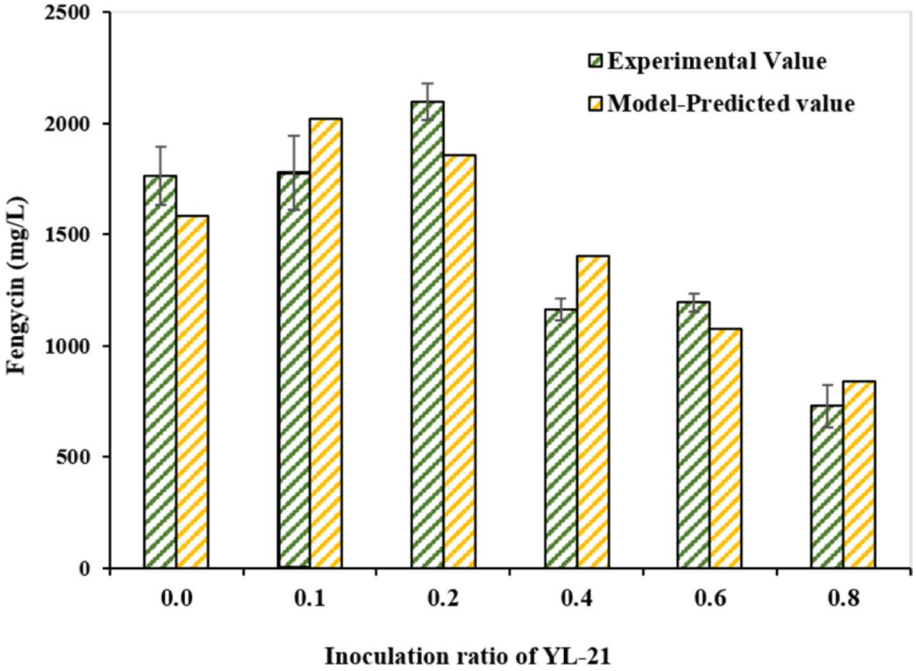

Fig. 8 Simulation results of fengycin production under the co-culture of strains CGF26-IV, Cgb-11, and YL-21. Data are presented as mean ± SD from three biologically independent samples

reached a relative error of 7.4% in ∞-norm sense, as shown in Figs. 6 and 7.

However, there were some differences between the predicted and observed peak values for the ratios and interval seeding times in various experiments. The reason for this discrepancy might be that the model is more adaptable to the system within certain ranges of proportions and times.

The effect of strain YL-21 inoculation size on fengycin production under three-strain artificial consortium of strain Cgb-11, YL-21 and CGF26-IV

In the artificial consortium of strains Cgb-11, YL-21, and CGF26-IV, fixing the optimal inoculation time and ratio of strains Cgb-11 and CGF26-IV, and simultaneously fixing the optimal inoculation time interval of strains YL-21 and CGF26-IV, in this case, we investigated the impact of different inoculation ratios of strain YL-21 on the fengycin production. The model achieved a relative error of 11.5% in ∞-norm sense, as shown in Fig. 8. For each experiment, we conducted fitting for the final fengycin yield. The overall fitting results were generally as expected.

Discussion

The multiple-strain artificial consortium is a multi-organism interaction system. The production of metabolic products is influenced by multiple factors, such as inoculation time and strain ratio. These characteristics can be naturally and suitably described by ODEs. Our goal is to extract key contributing factors and establish an appropriate kinetic model to elucidate the underlying biological mechanisms, which will be beneficial for guiding the experimental process and contributing to cost reduction.

During the model development phase, we constructed several ODEs. In addition to the model based on the Logistic equation presented in the main text, a Monod-based model (13) was also developed, which directly captures the interactions between microbial species, substrates, and metabolic products. Through numerical simulations, we evaluated the fitting performance of each model against experimental data and ultimately selected the previously introduced model (7–9):

$$\begin{cases} \frac{dX_1}{dt} = \mu_1(S)X_1 - \sigma_1 X_1, \\ \frac{dX_2}{dt} = \mu_2(S)X_2 - \sigma_2 X_2, \\ \frac{dS}{dt} = -\sigma_3\mu_1(S)X_1 - \sigma_4\mu_2(S)X_2, \\ \frac{dA}{dt} = \sigma_5\mu_2(S)X_2 - \sigma_6 A X_1, \\ \frac{dF}{dt} = \sigma_7 \cdot A \cdot S \cdot X_1. \end{cases} \tag{13}$$

However, our model and numerical simulations still exhibit significant limitations. On the one hand, our optimization model is built upon ODEs, but the feasible region for many parameters is difficult to estimate, and the mathematical properties of the optimization problem

have not been proved. These issues pose challenges for solving the optimization problem numerically. On the other hand, from the modeling perspective, the available biological data still suffer from several limitations. Many variables are difficult to measure directly, and even when measurements are taken, sampling errors may introduce noise, leading to a reduction in data volume and compromising data quality.

In summary, the current modeling framework still remains a certain gap for being directly applicable to experimental guidance. Moving forward, we plan to adopt more advanced optimization algorithms and incorporate GPU computation to enhance computational efficiency. Moreover, for achieving more robust and realistic simulation outcomes, stochastic differential equation (SDE) models will be explored by introducing randomness into the system.

Conclusions

In this study, we established a kinetic modeling framework based on ODEs to describe the production of fengycin in a multiple-strain artificial consortium. By fitting the model to experimental data, we obtained good agreement across diverse conditions, with fitting errors within about 7.4%–15.1%.

This work provides a unified and flexible framework for analyzing multiple-strain artificial consortiums, which is readily extendable to systems comprising N-strains. The model framework is adaptable and may contribute to optimize strain composition and process strategies in industrial bioproduction systems in the future.

Acknowledgements
The authors are grateful for the financial support from the National Key R&D Program of China (2018YFA0902200).

Author contributions
J.S.L.: conceptualization, methodology, investigation, validation, writing—original draft preparation, writing—review and editing. W.S.Y.: conceptualization, methodology, investigation, validation, writing—original draft preparation, writing—review and editing. G.G.R.: Conceptualization, methodology, investigation, validation. W.L.B.: investigation, validation. L.Z.X.: investigation, validation, writing—review and editing. Z.S.B.: methodology, investigation. L.X.: methodology, investigation. Q.X.H.: conceptualization, methodology. D.M.Z.: conceptualization, methodology, supervision, funding acquisition, writing—review and editing. Z.Y.: conceptualization, methodology, supervision, funding acquisition, writing—review and editing. C.J.S.: conceptualization, methodology, supervision, funding acquisition, writing—review and editing.

Funding
This study was funded by National Key R&D Program of China (2018YFA0902200).

Data availability
Data is provided within the manuscript or supplementary information files.

Declarations

Ethics approval and consent to participate
Not applicable.

Consent for publication
Not applicable.

Competing interests
The authors declare no competing interests.

Author details
[1]State Key Laboratory of Synthetic Biology, Tianjin University, Tianjin 300072, People's Republic of China. [2]School of Mathematics, Tianjin University, 92 Weijin Road, Nankai District, Tianjin 300072, People's Republic of China. [3]Frontiers Science Center for Synthetic Biology (Ministry of Education), School of Synthetic Biology and Biomanufacturing, Tianjin University, Tianjin 300072, People's Republic of China.

Received: 29 July 2025 Accepted: 25 December 2025
Published online: 27 January 2026

References

1. Deleu M, Paquot M, Nylander T. Effect of fengycin, a lipopeptide produced by *Bacillus subtilis*, on model biomembranes. Biophys J. 2008;94(7):2667–79.
2. Yan L, Li G, Liang Y, Tan MH, Fang JH, Peng JY, et al. Co-production of surfactin and fengycin by *Bacillus subtilis* BBW1542 isolated from marine sediment: a promising biocontrol agent against foodborne pathogens. J Food Sci Technol. 2024;61(3):563–72.
3. Raaijmakers JM, De Bruijn I, Nybroe O, Ongena M. Natural functions of lipopeptides from *Bacillus* and *Pseudomonas*: more than surfactants and antibiotics. FEMS Microbiol Rev. 2010;34:1037–62.
4. Lei LY, Xiong ZX, Li JL, Yang DZ, Li L, Chen L, et al. Biological control of *Magnaporthe oryzae* using natively isolated *Bacillus subtilis* G5 from *Oryza officinalis* roots. Front Microbiol. 2023;14:1264000.
5. Hammad M, Ali H, Hassan N, Tawab A, Salman M, Jawad I, et al. Food safety and biological control; genomic insights and antimicrobial potential of *Bacillus velezensis* FB2 against agricultural fungal pathogens. PLoS ONE. 2023;18(11):e0291975.
6. Yin Y, Wang X, Zhang P, Wang P, Wen J. Strategies for improving fengycin production: a review. Microb Cell Fact. 2024;23(1):144.
7. Tan W, Yin Y, Wen J. Increasing fengycin production by strengthening the fatty acid synthesis pathway and optimizing fermentation conditions. Biochem Eng J. 2022;177:108235.
8. Yaseen Y, Gancel F, Béchet M, Drider D, Jacques P. Study of the correlation between fengycin promoter expression and its production by *Bacillus subtilis* under different culture conditions and the impact on surfactin production. Arch Microbiol. 2017;199(10):1371–82.
9. Yaseen Y, Gancel F, Drider D, Béchet M, Jacques P. Influence of promoters on the production of fengycin in *Bacillus* spp. Res Microbiol. 2016;167(4):272–81.
10. Song HS, DeVilbiss F, Ramkrishna D. Modeling metabolic systems: the need for dynamics. Curr Opin Chem Eng. 2013;2(4):373–82.
11. Zheng Y, Sriram G. Mathematical modeling: bridging the gap between concept and realization in synthetic biology. J Biomed Biotechnol. 2010;2010:541609.
12. Laneras F, Picó J. Stoichiometric modelling of cell metabolism. J Biosci Bioeng. 2008;105(1):1–11.
13. Gernaey KV, Lantz AE, Tufvesson P, Woodley JM, Sin G. Application of mechanistic models to fermentation and biocatalysis for next-generation processes. Trends Biotechnol. 2010;28(7):346–54.
14. Mandli AR, Venkatesh KV, Modak JM. Constraints based analysis of extended cybernetic models. Biosystems. 2015;137:45–54.
15. Yasemi M, Jolicoeur M. Modelling cell metabolism: a review on constraint-based steady-state and kinetic approaches. Processes. 2021;9(2):322.
16. Sidorenko Y, Antoniukas L, Schulze-Horsel J, Kremling A, Reichl U. Mathematical model of growth and heterologous hantavirus protein production of the recombinant yeast *Saccharomyces cerevisiae*. Eng Life Sci. 2008;8(4):399–414.
17. Wu S, Xue Y, Yang S, Xu C, Liu C, Liu X, et al. Combinational quorum sensing devices for dynamic control in cross-feeding cocultivation. Metab Eng. 2021;67:186–97.

18. Medeot DB, Bertorello-Cuenca M, Liaudat JP, Alvarez F, Flores-Cáceres ML, Jofré E. Improvement of biomass and cyclic lipopeptides production in *Bacillus amyloliquefaciens* MEP218 by modifying carbon and nitrogen sources and ratios of the culture media. Biol Control. 2017;115(2):119–28.
19. Gao GR, Wei SY, Ding MZ, Hou ZJ, Wang DJ, Xu QM, et al. Enhancing fengycin production in the co-culture of *Bacillus subtilis* and *Corynebacterium glutamicum* by engineering proline transporter. Bioresour Technol. 2023;383:129229.
20. Levenspiel O. The Monod equation: a revisit and a generalization to product inhibition situations. Biotechnol Bioeng. 1980;22(8):1671–87.
21. Lotka AJ. Elements of physical biology. Williams & Wilkins; 1925.
22. Katoch S, Chauhan SS, Kumar V. A review on genetic algorithm: past, present, and future. Multimed Tools Appl. 2021;80:8091–126.
23. Lambora A, Gupta K, Chopra K. Genetic algorithm—a literature review. In: 2019 international conference on machine learning, big data, cloud and parallel computing (COMITCon). IEEE; 2019. p. 380–4.
24. Dormand JR, Prince PJ. A family of embedded Runge-Kutta formulae. J Comput Appl Math. 1980;6:19–26.
25. Gao GR, Hou ZJ, Ding MZ, Bai S, Wei SY, Qiao B, et al. Improved production of fengycin in *Bacillus subtilis* by integrated strain engineering strategy. ACS Synth Biol. 2022;11(12):4065–76.
26. Wang DJ, Ding MZ, Hou ZJ, Zhang Y, Shang W, Duan TX, Xu QM, Cheng JS. Carbon metabolism modification in *Bacillus subtilis* for improving fengycin production and investigating antifungal activity of its homologous components. ACS Synth Biol. 2025. https://doi.org/10.1021/acssynbio.5c00101
27. Li Q, Shang W, Sun H, Hou Z, Xu Q, Cheng J. ComQXPA quorum sensing dynamic regulation enhanced fengycin production of *Bacillus subtilis*. J Nat Prod. 2025;88(4):943–51.
28. Wei SY, Gao GR, Ding MZ, Cao CY, Hou ZJ, Cheng JS, et al. An engineered microbial consortium provides precursors for fengycin production by *Bacillus subtilis*. J Nat Prod. 2024;87(1):28–37.
29. Bai S, Qiao B, Hou ZJ, Gao GR, Cao CY, Cheng JS, et al. Mutualistic microbial community of *Bacillus amyloliquefaciens* and recombinant *Yarrowia lipolytica* co-produced lipopeptides and fatty acids from food waste. Chemosphere. 2023;310:136864.

Publisher's Note